ACS APPLIED MATERIALS & INTERFACES

Research Article

www.acsami.org

Cellulose Derived Graphenic Fibers for Capacitive Desalination of Brackish Water

Nalenthiran Pugazhenthiran,[†] Soujit Sen Gupta,[†] Anupama Prabhath,[†] Muthu Manikandan,[†] Jakka Ravindran Swathy,[†] V. Kalyan Raman,[‡] and Thalappil Pradeep*[,†]

[†]DST Unit of Nanoscience (DST UNS) and Thematic Unit of Excellence (TUE), Department of Chemistry, Indian Institute of Technology Madras, Chennai 600 036, India

[‡]Centre of Excellence (Biotechnology) & Water and Wastewater Technology, Thermax Limited, Pune 411019, India

Supporting Information

ABSTRACT: We describe a simple and inexpensive cellulose-derived and layer-by-layer stacked carbon fiber network electrode for capacitive deionization (CDI) of brackish water. The microstructure and chemical composition were characterized using spectroscopic and microscopic techniques; electrochemical/electrical performance was evaluated by cyclic voltammetry and 4-probe electrical conductivity and surface area by Brunauer–Emmett–Teller analysis, respectively. The desalination performance was investigated using a laboratory batch model CDI unit, under fixed applied voltage and varying salt concentrations. Electro-adsorption of NaCl on the graphite reinforced-cellulose (GrC) electrode reached equilibrium quickly (within 90 min) and the adsorbed salts were released swiftly (in 40 min) back into the solution, during reversal of applied potential. X-ray photoelectron spectroscopic studies clearly illustrate that sodium and chloride ions were physisorbed on the negative and positive electrodes, respectively during electro-adsorption. This GrC electrode showed an electro-adsorption capacity of 13.1 mg/g of the electrode at a cell potential of 1.2 V, with excellent recyclability and complete regeneration. The electrode has a high tendency for removal of specific anions, such as fluoride, nitrate, chloride, and sulfate from water in the following order: $Cl^- > NO_3^- > F^- > SO_4^{2-}$. GrC electrodes also showed resistance to biofouling with negligible biofilm formation even after 5 days of incubation in *Pseudomonas putida* bacterial culture. Our unique cost-effective methodology of layer-by-layer stacking of carbon nanofibers and concurrent reinforcement using graphite provides uniform conductivity throughout the electrode with fast electro-adsorption, rapid desorption, and extended reuse, making the electrode affordable for capacitive desalination of brackish water.

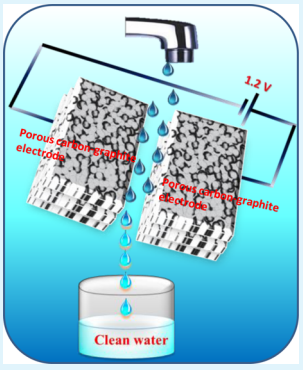

KEYWORDS: *capacitive deionization, graphene, nanofiber, adsorption, water purification*

INTRODUCTION

Shortage of clean water is the most exigent problem faced by several communities in the developing world. Access to safe and potable water is threatened by population growth, climate change, and contamination of existing fresh water sources.[1−3] The need for clean water for domestic, agricultural, and industrial processes has resulted in intense search for alternate sources of water supply, such as brackish groundwater and seawater.[1,3] Reverse osmosis (RO), ultrafiltration (UF), and distillation processes are the most widely used treatment technologies for water today.[4] However, excessive energy requirements and the need for skilled personnel to maintain such facilities are limiting their large scale deployment in resource-limited settings.[5]

Capacitive deionization (CDI) is increasingly being considered as a viable solution for water desalination that is more energy efficient than the above-mentioned processes. This technology fundamentally involves adsorption of oppositely charged ions from the electrical double layer region over an electrode upon application of a potential leading to desalination. Subsequent desorption of the adsorbed ions when the potential is reversed leads to regeneration of the electrodes.[5−9] Although CDI is associated with high theoretical efficiency, cost effectiveness, and point-of-use (POU) utility, its practical applications for desalination are yet to be realized fully.[6−10] The existing mainstream CDI materials with their inherent limitations in stability and resistance to biofouling confine such electrodes for larger scale operations. Various methods are used to solve these issues and commercial products are available; although capital costs are higher than RO. An ideal CDI material should exhibit the following characteristics: high specific surface area, high conductivity, fast adsorption/desorption rates, electrochemical stability, resistance to biofilm formation, and easy processability.[6,11,12]

The salt removal efficiency of various forms of carbon used as an electrode for CDI is generally reported in terms of salt (NaCl) adsorbed per gram of carbon. Li et al. and Kim et al. reported the capacity to be 0.275 and 3.7 mg/g, respectively for

Received: June 21, 2015
Accepted: August 25, 2015
Published: August 25, 2015

DOI: 10.1021/acsami.5b05510
ACS Appl. Mater. Interfaces 2015, 7, 20156−20163

Scheme 1. Schematic Representation of the Procedure for the Preparation of Layer-by-Layer Stacked Graphite-Reinforced-Carbon (GrC) Fiber Electrodes

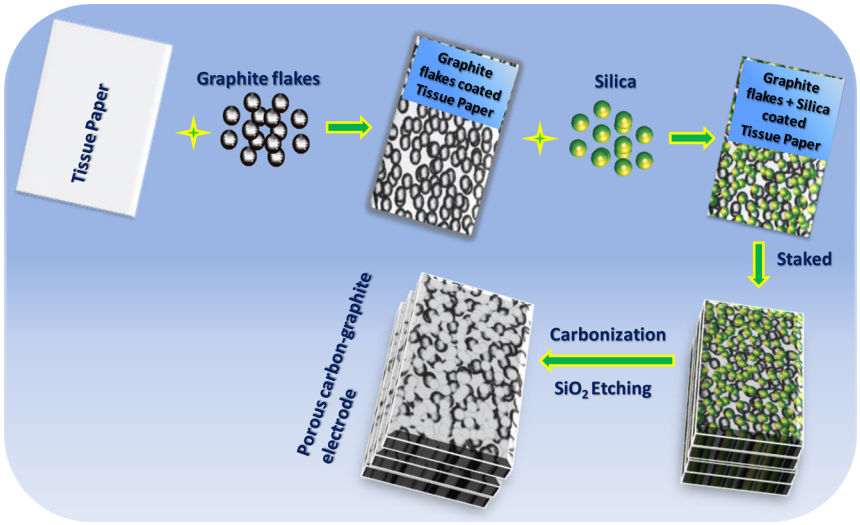

activated carbon.[13,14] In addition, multiwalled carbon nanotubes,[15] single-walled carbon nanotubes,[16] graphene-like nanoflakes,[17] graphene,[18] graphene-carbon nanotubes,[19] carbon nanofiber webs,[20] reduced graphene oxide-activated carbon,[21] Ti−O activated carbon cloth,[22] and MnO_2 activated carbon[23] have shown adsorption capacities of 1.7, 0.75, 1.3, 1.8, 1.4, 4.6, 2.9, 4.3, and 1.0 mg/g, respectively. These systems are excellent in terms of electrical conductivity and pore-distribution, but are found lacking in their symmetric adsorption and desorption of counterions, electrochemical stability, and resistance to biofouling. Additionally, they suffer from relatively complicated manufacturing processes and high production cost.[6] In comparison, mesoporous carbon is an inexpensive and highly porous material with varying pore sizes. This property can help overcome the limited ion accessibility and slow diffusion associated with activated carbon.[9,24−27] However, the obtained adsorption efficiency is less due to the high inner electrode resistance of reported mesoporous carbon materials.[24,26,28] Incorporation of conducting polymers, metal oxides, graphene and carbon nanotubes into mesoporous carbon is an effective approach for solving this issue.[25,29−34] Though these agents locally impart a pseudocapacitance on the surface, they do not contribute much to the adsorption efficiency. Recently, incorporating graphene into a mesoporous carbon increased its conductivity, as a result, it leads to higher adsorption of salt from brackish water compared to a carbon electrode alone.[13,21,35,36]

With an objective to develop a cost-effective and superior CDI electrode material with high surface area, low electrical resistance, and electrochemical durability, in this work we have synthesized a layer-by-layer stacked graphite reinforced-cellulose (GrC) derived 3D mesoporous fibrous carbon electrode. The material exhibits the above-mentioned characteristics along with superior adsorption capability and resistance to bacterial biofilm formation, while being cost-effective. The CDI performance of this hybrid electrode was evaluated and the effect of biofouling was examined via a temporal study employing a biofilm-forming organism, *Pseudomonas putida*. These characteristics make our graphite reinforced-cellulose derived carbon fiber material a promising candidate for POU water treatment, especially in resource-limited settings.

MATERIALS AND METHODS

Chemicals. Graphite flakes were a gift sample from Tamil Nadu Minerals Limited (TAMIN) and tissue papers were purchased from a local market in Chennai. Tetraethyl orthosilicate (TEOS) and 3-aminopropyltriethoxysilane (APTES) were purchased from Sigma-Aldrich and used as such. Unless otherwise specified, all the reagents used were of analytical grade and the solutions were prepared using deionized water.

Preparation of Layer-by-Layer Assembly of Graphite Reinforced-Carbon Electrode. The typical procedure for the preparation of a layer-by-layer assembly of a graphite reinforced-carbon (GrC) electrode was as follows (see Scheme 1). First, 5 mg of graphite (TAMIN) powder was coated on a single piece of tissue paper (size 5 × 5 cm and thickness of 0.2 mm) and then 300 μL of a TEOS:APTES mixture (ratio 1:0.5) was sprayed on it. This process was repeated for each layer (total 50 layers were prepared). Next, the entire set of graphite coated tissue paper layers were stacked on one above another and was pressed for 5 min (at 5 ton load) by a press. It was further dried at 60 °C for 3 h, which was followed by carbonization under nitrogen atmosphere at 700 °C for 3 h. After carbonization, silica was etched out from the stacked GrC electrode by aqueous NaOH (1 mM) for 3 h to generate pores. Finally, the electrode was washed with water several times until the pH of the mother liquor reached 7 and then dried overnight at 60 °C to remove water.

Capacitive Deionization Setup. The laboratory-scale CDI batch reactor consisted of a single pair of GrC electrodes and a pair of current collectors, as shown in Scheme 2. The current collectors were made of graphite rods and the electrodes were held at a spacing of ∼0.2 mm by a piece of nylon membrane. Power was supplied to the cell by connecting the current collectors to a direct-current (DC) Testtronic 30B DC power supply with a voltage range of 0−5 V and a current range of 0−1 A. The conductivity was measured at the cell exit stream by using a conductivity meter (cyberscan PCD 650 Eutech instrument). The approximate volume of the solution in the cell was 80 mL, which was maintained in the system. The temperature of the solution was kept at ∼25 °C. Regeneration of the electrodes was carried out by reversing the terminal of the electrodes.

Biofilm Formation. Monoculture biofilms of *Pseudomonas putida* were grown on the surface of the electrodes (a commercial electrode used for capacitive deionization and GrC). The protocol for the biofilm is reported elsewhere.[37] A few selected electrodes were immersed in 20 mL of a synthetic medium, inoculated with 10^8 colony forming units (CFU) of *Pseudomonas putida*. The biofilm was allowed to grow for 5 days while replenishment of the medium was done at an

DOI: 10.1021/acsami.5b05510
ACS Appl. Mater. Interfaces 2015, 7, 20156−20163

Scheme 2. Schematic Representation of the Capacitive Deionization Setup

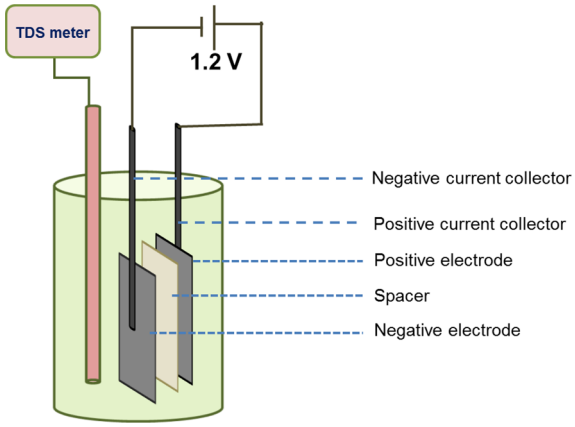

interval of 48 h. Electrodes after biofilm growth were rinsed in distilled water and air-dried for 24 h. The surfaces were sputtered with gold to increase their electrical conductivity before imaging. Scanning electron microscopy (SEM) studies were performed using a FEI QUANTA-200 operated at 12.5 kV.

Characterization Studies. Morphological studies of the electrode surface, elemental analysis, and elemental mapping were carried out using a scanning electron microscope equipped with energy dispersive analysis of X-rays (EDAX or energy dispersive spectroscopy, EDS) (FEI Quanta 200). The high resolution transmission electron microscopy (HRTEM) images of the electrodes were obtained with an instrument, JEM 3010 (JEOL, Japan) which was operated at 200 keV (to reduce beam induced damage) and the samples were drop-cast on carbon-coated copper grids and allowed to dry under ambient conditions. X-ray photoelectron spectroscopy (XPS) measurements were performed using ESCA Probe TPD of Omicron Nanotechnology with polychromatic Mg Kα as the X-ray source ($h\upsilon$ = 1253.6 eV) and the binding energy was calibrated with respect to C 1s at 284.5 eV. A Flowsorb II 2300 Micrometrics surface area analyzer was employed for measuring the surface area, pore volume, and pore diameter of the samples. Total sodium and chloride concentrations in the water were estimated using inductively coupled plasma spectroscopy (ICP-MS) (PerkinElmer NexION 300 ICP-MS) and ion chromatography (Metrohm 883 Basic IC plus), respectively. Raman spectra were obtained with a WITec GmbH, Alpha-SNOM alpha 300 S confocal Raman microscope having a 532 nm laser as the excitation source. The electrical conductivity was measured at room temperature by a four probe conductivity instrument (SES Instruments, Roorkee). A Keithley current source-voltmeter was attached to the four probe setup for the collection of data. The electrochemical capacitive behavior of CA was determined by cyclic voltammetry (CV). All electrochemical experiments were carried out at room temperature in a three-electrode cell with 1 M NaCl electrolyte solution.

RESULTS AND DISCUSSION

Characterization of Layer-by-Layer Stacked Assembly of Graphite Reinforced-Carbon (GrC) Electrode. To investigate the morphology of the GrC electrode, FESEM and HRTEM images were analyzed. Figure 1A,B,C shows that the prepared GrC electrodes are collectively intertwined in a unique fiber-like morphology with a thickness of 4−5 μm and a length of ten to several hundred micrometers. The graphite reinforcement into the consecutively stacked layer-by-layer assembly of carbon fiber is also evident from Figure 1A,B, marked in white arrows. This arrangement established an effective way for improving conductivity as well as mechanical strength. The material proved to be superior to similar carbon−carbon composites.[38−41] The elemental mapping confirmed the

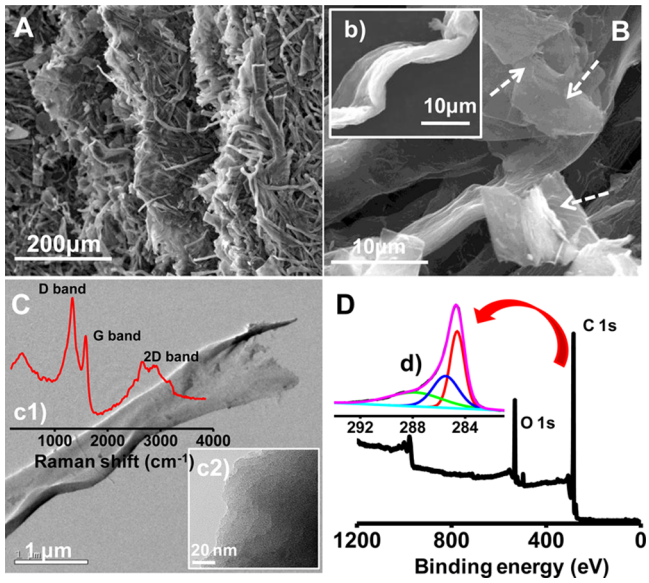

Figure 1. (A and B) FESEM images of layer-by layer stacked graphite reinforced carbon fiber. The white arrow in panel B shows the presence of graphite flakes. The inset in panel B represents the single layer graphenic carbon (b), (C) TEM image, the inset c1 represents the Raman spectrum of the material and c2 represents the HRTEM image of graphenic carbon, (D) XPS survey spectrum of the material and the inset shows the deconvoluted C 1s spectrum (d).

presence of silica in the initial material (Supporting Information, Figure S1). Figure S2 in the Supporting Information shows the complete etching of silica from the parent material, which led to the characteristic porosity of the GrC electrode. Furthermore, the Raman spectrum of the assembly in inset c1 in Figure 1C clearly shows that the material is graphenic in nature. The spectrum is composed of a primary in-plane vibrational mode at 1580 cm^{-1} (G band) and a second order overtone of a different in-plane vibration at 2690 cm^{-1} (2D band) and a defect band at 1350 cm^{-1} (D band).[42−44] This graphenic nature of the single carbon fiber represents multilayer graphene as shown in the HRTEM image in the inset of Figure 1C (c2). The X-ray photoelectron survey spectrum of GrC electrode (Figure 1D) shows the presence of carbon and oxygen as the only elements. The deconvoluted C 1s XPS (inset in Figure 1D) spectrum shows the presence of C═C at 284.6 eV and two "oxide" peaks that are shifted to higher binding energy by 1.0 and 1.5 eV, respectively. The first oxide peak is assigned to a carbon atom in alcohol (C—OH) or ether (C—O—C) groups. The second type of oxide corresponds to a C atom in carbonyl (C═O) type groups.

Structural properties (surface area and pore characteristic) and electrical conductivity have a major effect on the CDI performance of carbon materials. Therefore, the specific surface areas and the pore size distributions of the GrC electrode were measured using the BET and BJH methods. The nitrogen adsorption−desorption isotherms observed for the GrC electrode are shown in the Supporting Information, Figure S3. The calculated BET surface area and pore volume of the prepared samples are 598 m^2 g^{-1} and 0.358 cm^3 g^{-1}, respectively. The N_2 adsorption increased for P/P_0 > 0.1 owing to capillary condensation and multilayer adsorption of N_2 and the typical type-IV isotherm with H4 hysteresis loops indicate that the layer-by-layer assembly of carbon electrode is mesoporous in nature.[27,32,44] The BET isotherm results suggest

DOI: 10.1021/acsami.5b05510
ACS Appl. Mater. Interfaces 2015, 7, 20156−20163

that the GrC electrode is expected to be a potential candidate for salt adsorption from water in CDI.

Electrical conductivity of the material was around 128 S/m. It is postulated to be due to the layered structure of the electrode. The $I-V$ graph is shown in the Supporting Information, Figure S4A. Cyclic voltammerty was performed with GrC electrodes in a potential window of −0.8 to +0.2 V in 1 M NaCl solution as shown in the Supporting Information, Figure S4B. It is noted that at lower scan rates the curves are symmetrical, but at higher scan rates the curves distort. This can be attributed to the enhanced mass-transfer of the ions onto the GrC electrodes at lower scan rate but as the scan rate increases, the ohmic resistance also increases, which leads to the formation electrical double layer and thereby restricts the movement of the ions into the pores. The specific capacitances calculated using the CV curves were 323 and 83 F/g at 2 and 100 mV/s. The superior electrochemical property of the material enhances the electro-adsorption capacity of the GrC electrodes.

CDI Performance of the GrC Electrode. The CDI efficiency of the graphite reinforced-carbon electrode was evaluated using NaCl solution at room temperature with a single CDI cell (as depicted in Scheme 2) at an applied voltage of 1.2 V. Generally, water with total dissolved solids (TDS) higher than 500 mg/L is not considered suitable for consumption.[45] Bearing this in mind, we chose NaCl concentrations of 500 mg/L to test the CDI performance of these electrode materials. In Figure 2A, the NaCl electro-

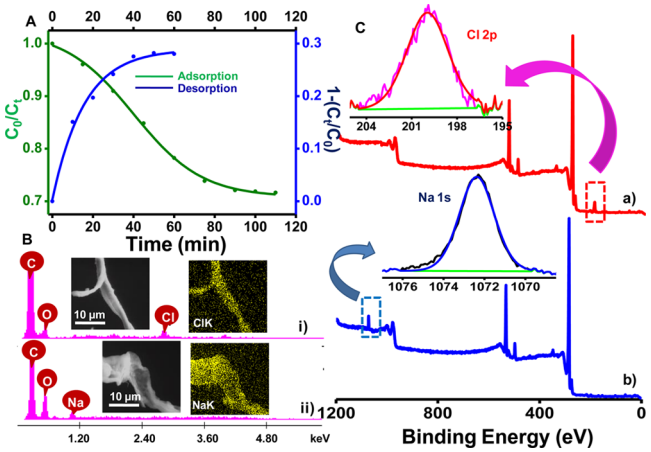

Figure 2. (A) Electro-adsorption/desorption curve of the graphite reinforced-carbon fiber electrode for a single cycle. The electrolyte present is NaCl measured at room temperature. (B) EDS spectra of (i) positive and (ii) negative terminals after single adsorption cycle. The corresponding SEM images along with the elemental maps are shown in the inset. (C) XPS survey spectrum of the material after single adsorption cycle, (a) positive and (b) negative terminals. The inset shows the deconvoluted XPS spectrum of Cl 2p and Na 1s.

adsorption and electro-desorption profiles of the electrode are plotted as a function of time. It is noticeable from the figure that the concentration of NaCl (500 mg/L) in the solution decreases gradually with time and reaches equilibrium. In comparison, when the potential was reversed, a rapid increase in NaCl concentration in solution occurs, which later stabilizes. One can further deduce from the electro-adsorption and electro-desorption profiles that ∼30% of NaCl is adsorbed in the first step, which is completely desorbed from the electrode on reversing the potential.[26,30,32,44] This implies that our porous carbon−graphite hybrid electrode can be regenerated efficiently.

The NaCl electro-adsorption capacity (q_e) of the electrodes is calculated from the following equation:

$$q_e = \frac{(C_0 - C_f)V}{W} \quad (1)$$

where C_0 and C_f are the initial and final NaCl concentrations (in mg/L) in solution, respectively, V is the volume (in mL) of the NaCl solution used, and W is the mass (in g) of the active material in the working electrode. The q_e of the graphite reinforced-carbon electrode was evaluated as 13.1 mg/g. Notably, the NaCl electro-adsorption capacity of the carbon−graphite hybrid electrode in this work is much higher than that of other recently reported CDI electrode materials, e.g., 0.731 mg/g for graphene incorporated-mesoporous carbon sheet.[7,34,46−50]

A fast electro-adsorption rate is also an important criterion responsible for allowing practical applications of CDI electrode materials. Various carbon based materials require several hours to reach their electro-adsorption equilibrium.[47,49] From the time dependent desalination behavior of the GrC electrode in Figure 2A, it is evident that the electro-adsorption of 500 mg/L NaCl reaches equilibrium quickly within 90 min, and the adsorbed salts are swiftly released back into the solution in 40 min during discharge compared to Li et al., which reported around 120 min for electro-adsorption.[13]

Elemental mapping and EDS analysis of the positive and negative electrodes are shown in Figure 2B and the Supporting Information, Figures S5 and S6. It clearly shows that the graphite reinforced-carbon electrodes have the capacity to remove salts from brackish water and get regenerated quickly. The XPS spectra of the positive and negative electrodes after application of potential are presented in Figure 2C. In comparison with Figure 1D, new peaks due to sodium and chloride ions adsorbed on the negative and positive electrode, respectively can be seen in the spectra. Interestingly, adsorption of these ions did not alter the binding energies of the carbon and oxygen peaks. This demonstrates that electro-adsorption of Na^+ and Cl^- ions on the electrodes is via physisorption alone.[42,51]

Studies were performed to investigate the reversibility of the GrC electrode during adsorption and regeneration. Figure 3A shows the ratio of initial concentration (C_0) to concentration at a time t (C_t) over several consecutive cycles. The symmetrical nature of the electro-adsorption (deionization) and desorption (regeneration) curves is characteristic of first-order kinetics associated with ion uptake and removal by the hybrid electrode.[52,53] The surface of the electrodes was characterized using XPS as shown in Figure 3B. Interestingly, there was no feature in the XPS spectrum corresponding to the negative and positive ions, and no shift in the binding energy of carbon and oxygen was observed. The EDS elemental mapping of the anode and cathode after the tenth adsorption cycle is shown in Figure 3C,D, and the corresponding EDS maps of the regenerated electrodes are shown in the Supporting Information, Figures S7 and S8. This study confirms that the GrC electrode maintains its adsorption and desorption capacity even after ten consecutive cycles. These results exhibit the high electro-adsorption capacity and a fast and reversible electro-adsorption/desorption.

DOI: 10.1021/acsami.5b05510
ACS Appl. Mater. Interfaces 2015, 7, 20156−20163

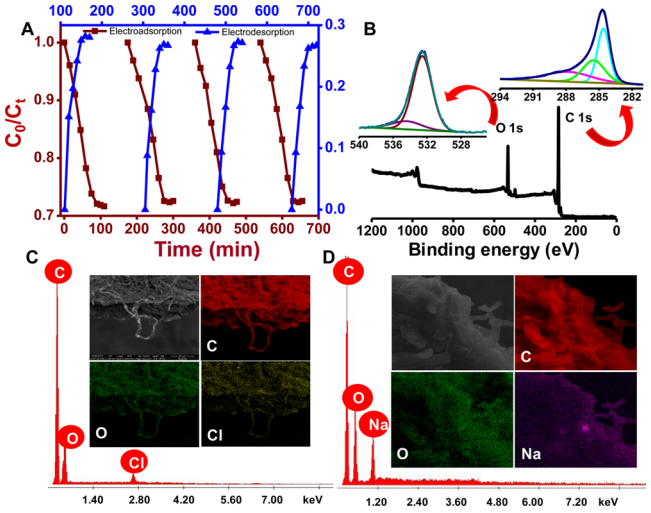

Figure 3. (A) Electro-adsorption/desorption cycles of the material (up to four cycles). (B) XPS spectrum of regenerated positive terminal after the tenth cycle showing the presence of carbon and oxygen only. The inset shows the deconvoluted C 1s and O 1s spectrum. (C and D) EDS spectra at the inset shows the SEM image and the corresponding elemental mapping for carbon, oxygen, and respective adsorbed ions. The electrolyte used in all cases was NaCl.

The electro-adsorption capacity is known to depend strongly on the surface properties, such as surface area, pore microstructure, and pore size distribution as well as solution state properties of the electrode material.[26,30,32,44,53] The layer-by-layer assembly of our GrC electrodes increases the mass-transfer of ions into the pores, ion electro-adsorption, and energy storage in the electrical double layer of the electrode. This consequently reduces the mass transport resistance of salt ions inside the electrode as well as between the electrode and saline water. This structural feature gives rise to a high electro-adsorption rate of the GrC electrodes and therefore, leads to excellent CDI performance.

The electro-adsorption capacity of the GrC electrodes was further investigated with respect to the effect of cation charge and size. For these solutions of NaCl, $MgCl_2$, and $FeCl_3$, each at an initial concentration of 500 ppm, were selected. The electro-adsorption and electro-desorption profiles of the GrC electrode for these solutions are compared with those of NaCl (500 ppm) in the Supporting Information, Figure S9. The concentrations of M^{x+} in solutions decrease with time and varies in the order $Fe^{3+} > Mg^{2+} > Na^+$ during the CDI experiment. The adsorption capacity was found to be 16.9, 14.5, and 13.1 mg/g for $FeCl_3$, $MgCl_2$, and NaCl, respectively. It is understandable that the ionic charge, ionic radii, and hydrated radii of different cations may play a major role in governing the electro-adsorption process. The hydrated radius of Fe^{3+} is the largest whereas that of Na^+ is the smallest in these cations, based on which the electro-adsorption preference should exhibit an opposite trend. The above order can instead be explained in terms of charge of the cations; as cations with higher charge will be more easily adsorbed on the electrode surface on application of a potential at the electrodes. Thus, the trivalent Fe^{3+} ion is most effectively removed, followed by the bivalent Mg^{2+} ion, and then the univalent Na^+ ion.[25,53] The GrC electrodes used in this study have a layer-by-layer assembly which allows the cations to move easily over the carbon–graphite electrode through the pores. This is confirmed from EDS coupled with elemental mapping analysis (Supporting Information, Figures S10–S13).

Anion contamination of both surface water and groundwater is well documented.[2,3,45] To test the effectiveness of our electrode for electro-adsorption of anions, several experiments were carried out using a solution containing different anions (such as SO_4^{2-}, Cl^-, NO_3^-, and F^-). The initial concentration of each of the selected anions was fixed at 50 ppm. About 2 mL aliquots of the analyte were withdrawn at regular intervals, and an analysis via ion chromatography was performed. Figure 4A

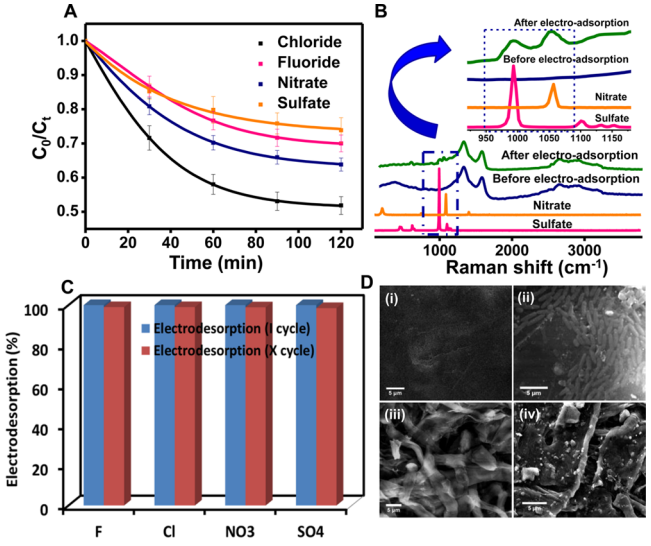

Figure 4. Plot of CDI performance of graphite reinforced carbon fiber electrode in the mixed negative ions (Cl^-, F^-, NO_3^-, SO_4^{2-}) system (A). Raman spectra of graphite reinforced carbon fiber electrode before and after electro-adsorption of positive electrode (B), inset shows enlarged Raman spectra of a narrower region. Plot of desorption capability of electrode in 1st and 10th cycle (C). SEM images of before and after 5 days growth of biofilms of *Pseudomonas putida* on commercial electrode (D(i,ii)) and graphite reinforced-carbon fiber electrode (D(iii,iv)).

shows that for each anion the concentration decreases with increase in time, indicating that they are adsorbed on the GrC electrode. These results were further confirmed through Raman spectroscopy (Figure 4B) and elemental mapping (Supporting Information, Figures S14 and S15). Raman spectra evidently indicate the presence of symmetric N–O and S–O stretching vibrations at 1056 and 990 cm^{-1} for nitrate and sulfate, respectively.[54] These features appeared clearly in the positive carbon–graphite electrode after electro-adsorption. Elemental mapping of positive and negative electrodes provide further evidence confirming electro-adsorption.

It can also be noticed from the adsorption profiles in Figure 4A that at a given time *t*, the measured anion concentration variation in solution follows the order: $Cl^- > NO_3^- > F^- > SO_4^{2-}$. The size of the hydrated radii of these anions decreases as $SO_4^{2-} > F^- > Cl^-, NO_3^-$. Anions with smaller hydrated radii can pass through the pores and arrive at the electrode surface more easily.[53,55,56] As a result, higher fractions of Cl^- and NO_3^- are removed than the other two anions. Finally, the recyclability of the GrC electrodes when treating water containing a mixture of anions was tested. We found negligible difference between the first and tenth cycles (Figure 4C), which indicateed that the electrodes were completely regenerated even after ten cycles.

DOI: 10.1021/acsami.5b05510
ACS Appl. Mater. Interfaces 2015, 7, 20156–20163

Further experiments were performed to test the efficiency of the GrC electrodes at different concentrations of NaCl solution (1000, 500, and 250 mg/L). In each case, we have found that the adsorption capacity of the electrodes is around 13.0 mg/g of material (keeping all other parameters constant). The graph is shown in the Supporting Information, Figure S16.

Biofouling of electrodes is a major issue impeding their utilization in the CDI process and is detrimental to their practical applications.[6] Though employing conventional biofouling control methods during capacitive desalination process can reduce biofouling of the electrodes, they also generate harmful byproducts requiring additional treatment.[57] In this context, we tested the effect of biofouling with *Pseudomonas putida* on the graphite reinforced-carbon fiber electrode. The SEM results (Figure 4D) showed that in comparison with a commercially available electrode, our graphite reinforced-carbon fiber electrode has an enhanced resistance to biofouling. This could be due to the graphenic nature of carbon fibers,[58] which have been individually proven to be effective antibacterial agents. The fiber-like surface morphology of the electrode could also provide it resistance against bacterial adhesion and proliferation. This is understandable because the surface charge of the carbon fiber-like structure may effectively repel bacteria from initial attachment on the GrC fiber electrode, thereby making it an effective material for long-term use.[57−59]

CONCLUSIONS

We have synthesized a graphite reinforced-cellulose derived carbon fiber electrode via a simple layer-by-layer stacking method. The reinforced graphite structure increases the conductivity of the electrode and results in excellent electro-adsorption of NaCl (13.1 mg/g). The high electro-adsorption performance is attributed to the layer-by-layer assembly of the hybrid electrode that allows ions to move easily on the carbon−graphite electrode. The graphenic carbon fiber-like surface morphology of the electrode could also provide it resistance against bacterial adhesion and proliferation. The preparation methodology of the carbon fiber electrode opens up a new avenue for the development of high-performance and cost-effective CDI electrodes from renewable sources.

ASSOCIATED CONTENT

Supporting Information

The Supporting Information is available free of charge on the ACS Publications website at DOI: 10.1021/acsami.5b05510.

BET surface area measurement of electrode and EDS coupled with elemental mapping analysis of electrode surface before and after electro-adsorption/desorption, I−V curve and CV curves of the GrC electrode at varying scan rates, CDI results of electro-adsorption and desorption performance of the GrC fiber electrode in different charged species ie., Na+, Mg2+ and Fe3+ and CDI performance of the GrC electrode at different NaCl concentration (PDF).

AUTHOR INFORMATION

Corresponding Author

*T. Pradeep. E-mail: pradeep@iitm.ac.in. Fax: +91-44-2257-0545.

Notes

The authors declare no competing financial interest.

ACKNOWLEDGMENTS

We thank the Department of Science and Technology and Nano Mission of Government of India for constantly supporting our research program on nanomaterials. S.S.G. thanks the SERB, CII, and Thermax India Pvt. Ltd. for a research fellowship.

REFERENCES

(1) Hoekstra, A. Y. Water Scarcity Challenges to Business. *Nat. Clim. Change* **2014**, *4*, 318−320.
(2) Schewe, J.; Heinke, J.; Gerten, D.; Haddeland, I.; Arnell, N. W.; Clark, D. B.; Dankers, R.; Eisner, S.; Fekete, B. M.; Colón-González, F. J.; Gosling, S. N.; Kim, H.; Liu, X.; Masaki, Y.; Portmann, F. T.; Satoh, Y.; Stacke, T.; Tang, Q.; Wada, Y.; Wisser, D.; Albrecht, T.; Frieler, K.; Piontek, F.; Warszawski, L.; Kabat, P. Multimodel Assessment of Water Scarcity under Climate Change. *Proc. Natl. Acad. Sci. U. S. A.* **2014**, *111*, 3245−3250.
(3) Shannon, M. A.; Bohn, P. W.; Elimelech, M.; Georgiadis, J. G.; Marinas, B. J.; Mayes, A. M. Science and Technology for Water Purification in the Coming Decades. *Nature* **2008**, *452*, 301−310.
(4) Elimelech, M.; Phillip, W. A. The Future of Seawater Desalination: Energy, Technology, and the Environment. *Science* **2011**, *333*, 712−717.
(5) Porada, S.; Weinstein, L.; Dash, R.; van der Wal, A.; Bryjak, M.; Gogotsi, Y.; Biesheuvel, P. M. Water Desalination Using Capacitive Deionization with Microporous Carbon Electrodes. *ACS Appl. Mater. Interfaces* **2012**, *4*, 1194−1199.
(6) Porada, S.; Zhao, R.; van der Wal, A.; Presser, V.; Biesheuvel, P. M. Review on the Science and Technology of Water Desalination by Capacitive Deionization. *Prog. Mater. Sci.* **2013**, *58*, 1388−1442.
(7) Suss, M. E.; Baumann, T. F.; Bourcier, W. L.; Spadaccini, C. M.; Rose, K. A.; Santiago, J. G.; Stadermann, M. Capacitive Desalination with Flow-Through Electrodes. *Energy Environ. Sci.* **2012**, *5* (11), 9511−9519.
(8) Suss, M. E.; Biesheuvel, P. M.; Baumann, T. F.; Stadermann, M.; Santiago, J. G. In Situ Spatially and Temporally Resolved Measurements of Salt Concentration between Charging Porous Electrodes for Desalination by Capacitive Deionization. *Environ. Sci. Technol.* **2014**, *48*, 2008−2015.
(9) Tsouris, C.; Mayes, R.; Kiggans, J.; Sharma, K.; Yiacoumi, S.; DePaoli, D.; Dai, S. Mesoporous Carbon for Capacitive Deionization of Saline Water. *Environ. Sci. Technol.* **2011**, *45*, 10243−10249.
(10) Długołęcki, P.; van der Wal, A. Energy Recovery in Membrane Capacitive Deionization. *Environ. Sci. Technol.* **2013**, *47*, 4904−4910.
(11) Oren, Y. Capacitive Deionization (CDI) for Desalination and Water Treatment — Past, Present and Future (a review). *Desalination* **2008**, *228*, 10−29.
(12) Zhao, R.; Biesheuvel, P. M.; Miedema, H.; Bruning, H.; van der Wal, A. Charge Efficiency: A Functional Tool to Probe the Double-Layer Structure Inside of Porous Electrodes and Application in the Modeling of Capacitive Deionization. *J. Phys. Chem. Lett.* **2010**, *1*, 205−210.
(13) Li, L.; Zou, L.; Song, H.; Morris, G. Ordered Mesoporous Carbons Synthesized by a Modified Sol−Gel process for Electrosorptive Removal of Sodium Chloride. *Carbon* **2009**, *47*, 775−781.
(14) Kim, Y.-J.; Choi, J.-H. Enhanced Desalination Efficiency in Capacitive Deionization with an Ion-Selective Membrane. *Sep. Purif. Technol.* **2010**, *71*, 70−75.
(15) Dai, K.; Shi, L.; Fang, J.; Zhang, D.; Yu, B. NaCl Adsorption in Multi-Walled Carbon Nanotubes. *Mater. Lett.* **2005**, *59*, 1989−1992.
(16) Li, H.; Pan, L.; Lu, T.; Zhan, Y.; Nie, C.; Sun, Z. A Comparative Study on Electrosorptive Behavior of Carbon Nanotubes and Graphene for Capacitive Deionization. *J. Electroanal. Chem.* **2011**, *653*, 40−44.
(17) Li, H.; Zou, L.; Pan, L.; Sun, Z. Novel Graphene-Like Electrodes for Capacitive Deionization. *Environ. Sci. Technol.* **2010**, *44*, 8692−8697.

DOI: 10.1021/acsami.5b05510
ACS Appl. Mater. Interfaces 2015, 7, 20156−20163

(18) Li, H.; Lu, T.; Pan, L.; Zhang, Y.; Sun, Z. Electrosorption Behavior of Graphene in NaCl Solutions. *J. Mater. Chem.* **2009**, *19*, 6773−6779.
(19) Zhang, D.; Yan, T.; Shi, L.; Peng, Z.; Wen, X.; Zhang, J. Enhanced Capacitive Deionization Performance of Graphene/Carbon Nanotube Composites. *J. Mater. Chem.* **2012**, *22*, 14696−14704.
(20) Wang, G.; Pan, C.; Wang, L.; Dong, Q.; Yu, C.; Zhao, Z.; Qiu, J. Activated Carbon Nanofiber Webs Made by Electrospinning for Capacitive Deionization. *Electrochim. Acta* **2012**, *69*, 65−70.
(21) Li, H.; Pan, L.; Nie, C.; Liu, Y.; Sun, Z. Reduced Graphene Oxide and Activated Carbon Composites for Capacitive Deionization. *J. Mater. Chem.* **2012**, *22*, 15556−15561.
(22) Ryoo, M.-W.; Seo, G. Improvement in Capacitive Deionization Function of Activated Carbon Cloth by Titania Modification. *Water Res.* **2003**, *37*, 1527−1534.
(23) Yang, J.; Zou, L.; Song, H.; Hao, Z. Development of Novel MnO2/Nanoporous Carbon Composite Electrodes in Capacitive Deionization Technology. *Desalination* **2011**, *276*, 199−206.
(24) Wang, X.; Lee, J. S.; Tsouris, C.; DePaoli, D. W.; Dai, S. Preparation of Activated Mesoporous Carbons for Electrosorption of Ions from Aqueous Solutions. *J. Mater. Chem.* **2010**, *20*, 4602−4608.
(25) Peng, Z.; Zhang, D.; Shi, L.; Yan, T. High Performance Ordered Mesoporous Carbon/Carbon Nanotube Composite Electrodes For Capacitive Deionization. *J. Mater. Chem.* **2012**, *22*, 6603−6612.
(26) Porada, S.; Borchardt, L.; Oschatz, M.; Bryjak, M.; Atchison, J. S.; Keesman, K. J.; Kaskel, S.; Biesheuvel, P. M.; Presser, V. Direct Prediction of the Desalination Performance of Porous Carbon Electrodes for Capacitive Deionization. *Energy Environ. Sci.* **2013**, *6*, 3700−3712.
(27) Peng, Z.; Zhang, D.; Shi, L.; Yan, T.; Yuan, S.; Li, H.; Gao, R.; Fang, J. Comparative Electroadsorption Study of Mesoporous Carbon Electrodes with Various Pore Structures. *J. Phys. Chem. C* **2011**, *115*, 17068−17076.
(28) Wang, G.; Qian, B.; Dong, Q.; Yang, J.; Zhao, Z.; Qiu, J. Highly Mesoporous Activated Carbon Electrode for Capacitive Deionization. *Sep. Purif. Technol.* **2013**, *103*, 216−221.
(29) Kim, Y.-J.; Choi, J.-H. Improvement of Desalination Efficiency in Capacitive Deionization using a Carbon Electrode Coated with an Ion-Exchange Polymer. *Water Res.* **2010**, *44*, 990−996.
(30) El-Deen, A. G.; Choi, J.-H.; Khalil, K. A.; Almajid, A. A.; Barakat, N. A. M. A TiO2 Nanofiber/Activated Carbon Composite as a Novel Effective Electrode Material for Capacitive Deionization of Brackish Water. *RSC Adv.* **2014**, *4*, 64634−64642.
(31) Kim, C.; Lee, J.; Kim, S.; Yoon, J. TiO2 Sol−Gel Spray Method for Carbon Electrode Fabrication to Enhance Desalination Efficiency of Capacitive Deionization. *Desalination* **2014**, *342*, 70−74.
(32) Wang, H.; Zhang, D.; Yan, T.; Wen, X.; Zhang, J.; Shi, L.; Zhong, Q. Three-Dimensional Macroporous Graphene Architectures as High Performance Electrodes for Capacitive Deionization. *J. Mater. Chem. A* **2013**, *1*, 11778−11789.
(33) Wang, H.; Shi, L.; Yan, T.; Zhang, J.; Zhong, Q.; Zhang, D. Design of Graphene-Coated Hollow Mesoporous Carbon Spheres as High Performance Electrodes for Capacitive Deionization. *J. Mater. Chem. A* **2014**, *2*, 4739−4750.
(34) Li, H.; Liang, S.; Li, J.; He, L. The Capacitive Deionization Behaviour of a Carbon Nanotube and Reduced Graphene Oxide Composite. *J. Mater. Chem. A* **2013**, *1*, 6335−6341.
(35) Bai, Y.; Huang, Z.-H.; Yu, X.-L.; Kang, F. Graphene Oxide-Embedded Porous Carbon Nanofiber Webs by Electrospinning for Capacitive Deionization. *Colloids Surf., A* **2014**, *444*, 153−158.
(36) Liu, Y.; Xu, X.; Lu, T.; Sun, Z.; Chua, D. H. C.; Pan, L. Nitrogen-Doped Electrospun Reduced Graphene Oxide-Carbon Nanofiber Composite for Capacitive Deionization. *RSC Adv.* **2015**, *5*, 34117−34124.
(37) Sutherland, I. W. The Biofilm Matrix − An Immobilized but Dynamic Microbial Environment. *Trends Microbiol.* **2001**, *9* (5), 222−227.
(38) Fitzer, E.; Terwiesch, B. Carbon—Carbon Composites Unidirectionally Reinforced with Carbon and Graphite Fibers. *Carbon* **1972**, *10*, 383−390.
(39) Fitzer, E. The Future of Carbon-Carbon Composites. *Carbon* **1987**, *25*, 163−190.
(40) Windhorst, T.; Blount, G. Carbon-Carbon Composites: A Summary of Recent Developments and Applications. *Mater. Eng.* **1997**, *18*, 11−15.
(41) Manocha, L. M.; Yasuda, E.; Tanabe, Y.; Kimura, S. Effect of Carbon Fiber Surface-Treatment on Mechanical Properties of C/C Composites. *Carbon* **1988**, *26*, 333−337.
(42) Sreeprasad, T. S.; Gupta, S. S.; Maliyekkal, S. M.; Pradeep, T. Immobilized Graphene-Based Composite from Asphalt: Facile Synthesis and Application in Water Purification. *J. Hazard. Mater.* **2013**, *246−247*, 213−220.
(43) John, R.; Shinde, D. B.; Liu, L.; Ding, F.; Xu, Z.; Vijayan, C.; Pillai, V. K.; Pradeep, T. Sequential Electrochemical Unzipping of Single-Walled Carbon Nanotubes to Graphene Ribbons Revealed by in Situ Raman Spectroscopy and Imaging. *ACS Nano* **2014**, *8*, 234−242.
(44) Wen, X.; Zhang, D.; Yan, T.; Zhang, J.; Shi, L. Three-Dimensional Graphene-Based Hierarchically Porous Carbon Composites Prepared by a Dual-Template Strategy for Capacitive Deionization. *J. Mater. Chem. A* **2013**, *1*, 12334−12344.
(45) Sankar, M. U.; Aigal, S.; Maliyekkal, S. M.; Chaudhary, A.; Anshup; Kumar, A. A.; Chaudhari, K.; Pradeep, T. Biopolymer-Reinforced Synthetic Granular Nanocomposites for Affordable Point-of-Use Water Purification. *Proc. Natl. Acad. Sci. U. S. A.* **2013**, *110*, 8459−8464.
(46) Li, H.; Zaviska, F.; Liang, S.; Li, J.; He, L.; Yang, H. Y. A High Charge Efficiency Electrode by Self-Assembling Sulphonated Reduced Graphene Oxide onto Carbon Fibre: Towards Enhanced Capacitive Deionization. *J. Mater. Chem. A* **2014**, *2*, 3484−3491.
(47) El-Deen, A. G.; Barakat, N. A. M.; Khalil, K. A.; Kim, H. Y. Development of Multi-Channel Carbon Nanofibers as Effective Electrosorptive Electrodes for a Capacitive Deionization Process. *J. Mater. Chem. A* **2013**, *1*, 11001−11010.
(48) Zhang, D.; Wen, X.; Shi, L.; Yan, T.; Zhang, J. Enhanced Capacitive Deionization of Graphene/Mesoporous Carbon Composites. *Nanoscale* **2012**, *4*, 5440−5446.
(49) Wen, X.; Zhang, D.; Shi, L.; Yan, T.; Wang, H.; Zhang, J. Three-Dimensional Hierarchical Porous Carbon with a Bimodal Pore Arrangement for Capacitive Deionization. *J. Mater. Chem.* **2012**, *22*, 23835−23844.
(50) Pasta, M.; Wessells, C. D.; Cui, Y.; La Mantia, F. A Desalination Battery. *Nano Lett.* **2012**, *12*, 839−843.
(51) Maliyekkal, S. M.; Sreeprasad, T. S.; Krishnan, D.; Kouser, S.; Mishra, A. K.; Waghmare, U. V.; Pradeep, T. Graphene: A Reusable Substrate for Unprecedented Adsorption of Pesticides. *Small* **2013**, *9*, 273−283.
(52) Mossad, M.; Zou, L. Evaluation of the Salt Removal Efficiency of Capacitive Deionisation: Kinetics, Isotherms and Thermodynamics. *Chem. Eng. J.* **2013**, *223* (0), 704−713.
(53) Mossad, M.; Zou, L. A Study of the Capacitive Deionisation Performance under Various Operational Conditions. *J. Hazard. Mater.* **2012**, *213-214*, 491−497.
(54) Dudik, J. M.; Johnson, C. R.; Asher, S. A. Wavelength Dependence of the Preresonance Raman Cross Sections of CH3CN, SO42−, ClO4−, and NO3−. *J. Chem. Phys.* **1985**, *82*, 1732−1740.
(55) Pan, L.; Li, H.; Zhan, Y.; Zhang, Y.; Sun, Z. Electrosorption Behavior of Carbon Nanotube and Carbon Nanofiber Film Electrodes. *Curr. Phys. Chem.* **2011**, *1*, 16−26.
(56) Pan, L.; Wang, X.; Gao, Y.; Zhang, Y.; Chen, Y.; Sun, Z. Electrosorption of Anions with Carbon Nanotube and Nanofibre Composite Film Electrodes. *Desalination* **2009**, *244*, 139−143.
(57) Nguyen, T.; Roddick, F.; Fan, L. Biofouling of Water Treatment Membranes: A Review of the Underlying Causes, Monitoring Techniques and Control Measures. *Membranes* **2012**, *2*, 804−840.

DOI: 10.1021/acsami.5b05510
ACS Appl. Mater. Interfaces 2015, 7, 20156−20163

(58) Chen, J.; Peng, H.; Wang, X.; Shao, F.; Yuan, Z.; Han, H. Graphene Oxide exhibits Broad-Spectrum Antimicrobial Activity against Bacterial Phytopathogens and Fungal Conidia by Intertwining and Membrane Perturbation. *Nanoscale* **2014**, *6*, 1879−1889.
(59) Mansouri, J.; Harrisson, S.; Chen, V. Strategies for Controlling Biofouling in Membrane Filtration Systems: Challenges and Opportunities. *J. Mater. Chem.* **2010**, *20*, 4567−4586.

DOI: 10.1021/acsami.5b05510
ACS Appl. Mater. Interfaces 2015, 7, 20156−20163